# Polarization of a probe laser beam due to nonlinear QED effects

Soroush Shakeri,[1,2,*] Seyed Zafarollah Kalantari,[1,†] and She-Sheng Xue[2,3,‡]
[1]*Department of Physics, Isfahan University of Technology, Isfahan 84156-83111, Iran*
[2]*ICRANet Piazzale della Repubblica, 10-65122, Pescara, Italy*
[3]*Physics Department, University of Rome La Sapienza, Piazzale le Aldo Moro 5, I00185 Rome, Italy*
(Received 2 September 2016; published 9 January 2017)

Nonlinear QED interactions induce different polarization properties on a given probe beam. We consider the polarization effects caused by the photon-photon interaction in laser experiments, when a laser beam propagates through a constant magnetic field or collides with another laser beam. We solve the quantum Boltzmann equation within the framework of the Euler-Heisenberg Lagrangian for both time-dependent and constant background field to explore the time evolution of the Stokes parameters $Q$, $U$, and $V$ describing polarization. Assuming an initially linearly polarized probe laser beam, we also calculate the induced ellipticity and rotation of the polarization plane.

DOI: 10.1103/PhysRevA.95.012108

## I. INTRODUCTION

The strong-field regime of QED is a completely new area of physics with new phenomena such as "nonlinear QED effects"; these features will be tested by ongoing experiments. The QED quantum vacuum made up of virtual pairs, when exposed to intense light, effectively behaves as a birefringent medium [1–4], due to nonlinear interactions introduced into the linear Maxwell equation. Recently, there have been many experimental efforts to detect photon-photon interactions [5–10]; the direct evidence of elastic scattering has not been observed yet. These experiments are mainly based on ellipticity induced in an initially linearly polarized probe laser passing through a background field, provided by superconducting magnets [7–10] or high intensity lasers [5,6,11,12] in analogy to a beam of light passing through a birefringent crystal. This means we have two cases for analysis: (1) the laser propagation through a static magnetic field made by ground magnets and (2) the collision between two laser beams in which one of the laser beams behaves as an electromagnetic background for another one.

In order to observe the QED nonlinearities for weak fields in the laboratory, long interaction length or time is required. In these kinds of experiments [7–9], there is an interaction of optical laser photons, which are highly linearly polarized, with the magnetic-field strength of the order of a few tesla. By contrast, upcoming high intensity laser systems will be able to achieve ultra-high-field strengths in the laboratory [11,13–15]. The current laser intensity record (in the optical regime) is given by $2 \times 10^{22}$ W/cm$^2$ [16] and future facilities envisage even higher intensities of the order of $10^{24}$–$10^{25}$ W/cm$^2$ [6]. Because of this drastic enhancement of field strengths, it is possible to probe distances of about electron Compton wavelength where the quantum effects play an important role [14]. There is a critical electric field $E_{\rm cr} = 1.3 \times 10^{16}$ V/cm, in which an electron gains an energy $m_e$ upon traveling a distance equal to its Compton wavelength [14,15,17]. In such a field it becomes energetically favorable to produce real electron-positron pairs from the vacuum [2,4,18,19], and correspondingly a critical magnetic field $B_{\rm cr} = 4.4 \times 10^{13}$ G. In [20–22] there are some proposals to measure QED nonlinearities, especially in [21], where by using combined optical and x-ray lasers, due to the birefringence effect, QED nonlinearities increase with background field strength and probe beam frequency. This scenario will be realized with the Helmholtz international beamline for extreme fields (HIBEF) facility employing the European x-ray free electron laser (XFEL) at DESY [5], and will, if successful, give the first experimental verification of vacuum birefringence along with photon-photon scattering.

However, it is not clear if one gets the same results from the experiments in the static strong-field or time-dependent one. The laser beam consists of oscillating electric and magnetic fields, and the authors of [20,21] have proposed that a standing wave generated by the superposition of two counterpropagating strong and tightly focused optical laser beams can be used as a target for a given x-ray probe beam. Although in principle it is possible to set up high-power short pulse-laser standing waves, this would not be easily achieved in practice. In this paper, in addition to the static strong field, we consider a time-dependent field configuration which occurs in the cross region of two laser beams the frequencies of which are different. The aims of this paper are (i) presenting a quantum-mechanical description for the generation of an ellipticity signal in both constant and time-varying background fields; (ii) investigating observational consequence and discrepancy of these two cases; and (iii) considering the effects of both time-varying electric and magnetic fields on the polarization characteristics of a given probe beam. For these purposes, we use the generalized quantum Boltzmann equation formulated in [23,24], to study the evolution of polarization characteristics for a probe beam propagating through background fields. In this paper we have extended the recent study [22] to provide more details of the different experimental setups in more realistic configurations. This paper is organized as follows. In Sec. II, we review prescription of the polarization by Stokes parameters and relating to ellipticity and rotation of polarization plane angles, and the evolution in time obeying the quantum Boltzmann equation. In Sec. III, we examine the generation of polarization characteristics of the probe beam in the presence of the background fields,

*soroush.shakeri@ph.iut.ac.ir
†zafar@cc.iut.ac.ir
‡xue@icra.it

 

taking into account the Euler-Heisenberg effective Lagrangian. In Sec. IV, we obtain the set of equations governing the time evolution of the Stokes parameters. We analytically and numerically solve these equations to obtain polarization characteristics of the probe beam in both cases of time-dependent and static background fields. Finally, in the last section after some discussions, we give some concluding remarks.

## II. FARADAY ROTATION, STOKES PARAMETERS, AND THE BOLTZMANN EQUATION

We consider a monochromatic electromagnetic wave propagating in the $\hat{z}$ direction, where the electric and magnetic fields oscillate in the $x$-$y$ plane. At a spatial point, the electric-field vector can be written as

$$\vec{E} = E_x\hat{x} + E_y\hat{y} = (E_{0x}e^{i\phi_x}\hat{x} + E_{0y}e^{i\phi_y}\hat{y})e^{-i\omega t} \quad (1)$$

where $\phi_x$ and $\phi_y$ are the phases at the initial time, and $E_{0x}$ and $E_{0y}$ are amplitudes in the $\hat{x}$ and $\hat{y}$ directions. Polarization properties are normally described in terms of the Stokes parameters: the total intensity $I$, linear polarization $Q$ and $U$, and the circular polarization $V$. They are defined as time-averaged quantities [23–26]:

$$I \equiv \langle E_x^2\rangle + \langle E_y^2\rangle, \quad (2)$$

$$Q \equiv \langle E_x^2\rangle - \langle E_y^2\rangle, \quad (3)$$

$$U \equiv \langle 2E_xE_y\cos(\phi_x - \phi_y)\rangle, \quad (4)$$

$$V \equiv \langle 2E_xE_y\sin(\phi_x - \phi_y)\rangle. \quad (5)$$

$Q$ and $U$ depend on the orientation of the coordinate system on the plane orthogonal to the direction of propagation, whereas $I$ and $V$ are independent of this coordinate system [23].

Alternatively, linearly polarized light can be considered as a superposition of two opposite circular polarized waves,

$$\vec{E} = E_R\hat{R} + E_L\hat{L} = (E_{0R}e^{i\phi_R}\hat{R} + E_{0L}e^{i\phi_L}\hat{L})e^{-i\omega t}, \quad (6)$$

where $\hat{R}(\hat{L})$ stands for unit vectors for the right-hand (left-hand) polarization. According to this redefinition $Q$ and $U$ can be expressed as

$$Q \equiv \langle 2E_RE_L\cos(\phi_R - \phi_L)\rangle, \quad (7)$$

$$U \equiv \langle 2E_RE_L\sin(\phi_R - \phi_L)\rangle. \quad (8)$$

If a wave propagates through a magnetized plasma, its polarization vectors will rotate. Then the net rotation of the plane of polarization is $\Delta\phi_{\rm FR} = \frac{1}{2}(d\phi_L - d\phi_R) = (k_L - k_R)dz$; this phenomenon is called Faraday rotation (FR). This phase shift mixes $Q$ and $U$ parameters such as

$$\dot{Q} = -2U\frac{d\Delta\phi_{\rm FR}}{dt}, \quad (9)$$

$$\dot{U} = -2Q\frac{d\Delta\phi_{\rm FR}}{dt}. \quad (10)$$

On the other hand, when linear polarized light with circular polarized normal modes passes through an optically active sample with a different absorbance for different components (refer to the imaginary part of a medium's refractive index), circular polarized light is a consequence of this absorbance. For an initially linearly polarized wave with linear components as normal modes like Eq. (1), in contrast to decomposition to the circular states, the difference in phase velocities $\phi_x - \phi_y$ leads to a mixing between $U$ and $V$ parameters

$$\dot{V} = 2U\frac{d\Delta\phi_{\rm FC}}{dt}, \quad (11)$$

which measures the angle related to Faraday conversion (FC) in a magnetized medium [26].

The quantum vacuum in the background fields effectively behaves as a birefringence medium, introducing a Faraday rotation (circular birefringence) on the light beam passing through it [10]. The complex index of refraction is written as $\tilde{n} = n + i\kappa$, where $n$ is the index of refraction and $\kappa$ is the extinction coefficient. A linear birefringence can be described as the difference between the real refraction indices for the two polarizations $\Delta n = n_\parallel - n_\perp$, where $n_\parallel$ is parallel to the optical axis (in our case the magnetic-field direction) and $n_\perp$ is perpendicular to it. Similarly, a dichroism can be defined as the difference in extinction coefficient $\Delta\kappa = \kappa_\parallel - \kappa_\perp$ [7]. During propagation along a path with length $L$, a birefringence $\Delta n$ and a dichroism $\Delta\kappa$ generate an ellipticity $\epsilon$ and a rotation angle of the major axis of the ellipse $\psi$, respectively, which are represented by

$$\epsilon = \frac{\pi\Delta nL}{\lambda}\sin 2\vartheta, \quad (12)$$

$$\psi = \frac{\pi\Delta\kappa L}{\lambda}\sin 2\vartheta, \quad (13)$$

where $\vartheta$ is the angle between the light polarization vector and the optical axis direction. The Stokes parameters can be related to the polarization rotation angle ($\psi$) and ellipticity angle ($\epsilon$) [27]:

$$I = I_0, \quad (14)$$

$$Q = I_0\cos 2\epsilon\cos 2\psi, \quad (15)$$

$$U = I_0\cos 2\epsilon\sin 2\psi, \quad (16)$$

$$V = I_0\sin 2\epsilon, \quad (17)$$

where $I_0$, $2\psi$, and $2\epsilon$ are the spherical coordinates of the three-dimensional vector of Cartesian coordinates $(Q,U,V)$. Since the three parameters $I_0$, $2\psi$, and $2\epsilon$ determine the four Stokes parameters, there must be a relation between the Stokes parameters; this relation is $I^2 = Q^2 + U^2 + V^2$ (only true for the 100% polarized light). For a general source of light which is a superposition of many different waves without any fixed phase relation between them, all four Stokes parameters are independent of each others and should be measured separately, in this case $I^2 \geqslant Q^2 + U^2 + V^2$. However, for given sets of Stokes parameters, one can transform the spherically

coordinate Eqs. (14)–(17) to obtain the following relations:

$$I = I_0, \tag{18}$$

$$2\psi = \arctan\left(\frac{U}{Q}\right), \tag{19}$$

$$2\epsilon = \arctan\left(\frac{V}{\sqrt{Q^2+U^2}}\right). \tag{20}$$

Generally if one has a polarization ellipse that the electric-field end point traces out, $\psi$ represents the angle of the polarization plane and $\epsilon$ manifests its ellipticity.

The Stokes parameters can be defined in a quantum-mechanical description by using the quantum operators and states in which the linear basis corresponds to Stokes parameters [23,24]. In a general mixed state, an ensemble of photons can be described by a normalized density matrix $\rho_{ij} \equiv (|\epsilon_i\rangle\langle\epsilon_j|/\mathrm{tr}\rho)$. The density matrix $\rho$ on the polarization state space encodes the intensity and polarization of the photon ensemble; the expectation value for the Stokes parameters is given by

$$I \equiv \langle\hat{I}\rangle = \mathrm{tr}\rho\hat{I} = \rho_{11} + \rho_{22}, \tag{21}$$

$$Q \equiv \langle\hat{Q}\rangle = \mathrm{tr}\rho\hat{Q} = \rho_{11} - \rho_{22}, \tag{22}$$

$$U \equiv \langle\hat{U}\rangle = \mathrm{tr}\rho\hat{U} = \rho_{12} + \rho_{21}, \tag{23}$$

$$V \equiv \langle\hat{V}\rangle = \mathrm{tr}\rho\hat{V} = i(\rho_{12} - \rho_{21}). \tag{24}$$

These relations show that the density matrix for a system of photons contains the same information as the four Stokes parameters. The explicit expression of the density matrix in the linear polarization basis in terms of Stokes parameters is given as follows:

$$\rho = \frac{1}{2}\begin{pmatrix} I+Q & U-iV \\ U+iV & I-Q \end{pmatrix}. \tag{25}$$

In fact, one can evaluate the time evolution of the polarization vectors by considering the time evolution of the density matrix. The density operator $\hat{\rho}$ for an ensemble of free photons is given by

$$\hat{\rho} = \int \frac{d^3p}{(2\pi)^3}\rho_{ij}(p)\hat{a}_i^\dagger(p)\hat{a}_j(p), \tag{26}$$

where the density matrix elements $\rho_{ij}$ are related to the number operators $\hat{\mathcal{D}}_{ij}(\mathbf{k}) = \hat{a}_i^\dagger(\mathbf{k})\hat{a}_j(\mathbf{k})$ as follows:

$$\langle\hat{\mathcal{D}}_{ij}(\mathbf{k})\rangle = (2\pi)^3 2k^0\delta^{(3)}(0)\rho_{ij}(\mathbf{k}). \tag{27}$$

The time evolution of the photon number operator can be given as

$$\frac{d}{dt}\hat{\mathcal{D}}_{ij} = i[\hat{H},\hat{\mathcal{D}}_{ij}], \tag{28}$$

$$\left\langle\frac{d}{dt}\hat{\mathcal{D}}_{ij}\right\rangle(t) \simeq i\langle[\hat{\mathcal{H}}_{\mathrm{int}},\hat{\mathcal{D}}_{ij}]\rangle - \int_0^t dt'\langle[\hat{\mathcal{H}}_{\mathrm{int}}(t-t'),[\hat{\mathcal{H}}_{\mathrm{int}}(t'),\hat{\mathcal{D}}_{ij}]]\rangle, \tag{29}$$

where $\hat{H}$ is the total Hamiltonian and $\hat{\mathcal{H}}_{\mathrm{int}}$ is the interacting Hamiltonian. Equation (29) can be expressed in terms of the density matrix [24]

$$(2\pi)^3 2k^0\delta^{(3)}(0)\frac{d}{dt}\rho_{ij}(\mathbf{k}) = i\langle[\hat{\mathcal{H}}_{\mathrm{int}}(t),\hat{\mathcal{D}}_{ij}(\mathbf{k})]\rangle - \frac{1}{2}\int_{-\infty}^{+\infty} dt\langle[\hat{\mathcal{H}}_{\mathrm{int}}(t),[\hat{\mathcal{H}}_{\mathrm{int}}(0),\hat{\mathcal{D}}_{ij}(\mathbf{k})]]\rangle. \tag{30}$$

Equation (30) is called the quantum Boltzmann equation, and the time evolution of the Stokes parameters is given by this equation; the first term on the right-hand side is referred to as the forward-scattering term while the second one is the usual collision term. In the case of linear Maxwellian electrodynamics, the time evolution of the Stokes parameter $V$ is always equal to zero, and no circular polarization occurs. In the following section, we will show that if nonlinear QED interaction in the presence of strong background fields is included the time evolution of $V$ does not vanish, leading to nonzero circular polarization. According to Eqs. (20) and (19), the time dependence of $V$, $U$, and $Q$ parameters gives rise to the variation of ellipticity $\epsilon$ and a rotation of polarization plane $\psi$ which are principally measurable quantities in laser experiments.

## III. EULER-HEISENBERG LAGRANGIAN AND THE GENERATION OF CIRCULAR POLARIZATION IN THE PRESENCE OF BACKGROUND FIELDS

Here we are going to consider the nonlinear QED process in the strong background fields which are provided by superconducting magnets or by an ultraintense laser. In fact an intense laser field represents a photon coherent state with a large number of photons. In a typical petawatt class laser there are $10^{18}$ photons in a cubic laser wavelength; the correspondence principle tells us this laser beam is very well behaved like classical electromagnetic fields [18]. In the following, we adopt the effective Euler-Heisenberg Lagrangian at the level of one-loop calculation [2,28–30]

$$\mathcal{L}_{\mathrm{eff}} = -\frac{1}{4}\mathcal{F}_{\mu\nu}\mathcal{F}^{\mu\nu} + \frac{1}{180}\frac{\alpha^2}{m_e^4}[5(\mathcal{F}_{\mu\nu}\mathcal{F}^{\mu\nu})^2 - 14\mathcal{F}_{\mu\nu}\mathcal{F}^{\nu\lambda}\mathcal{F}_{\lambda\rho}\mathcal{F}^{\rho\mu}], \tag{31}$$

where the first term is the classical Maxwell Lagrangian, $m_e$ is the electron mass, and $\alpha$ is the fine-structure constant. In the Euler-Heisenberg Lagrangian the photon interactions in the presence of a background field can be considered by replacing $\mathcal{F}_{\mu\nu} \to f_{\mu\nu} + F_{\mu\nu}$ with the probe quantum field $f_{\mu\nu}$ as a weak perturbation on top of the strong background field $F_{\mu\nu}$, which varies slowly in comparison with $f_{\mu\nu}$. The quantum field $f_{\mu\nu} = \partial_\mu\hat{A}_\nu - \partial_\nu\hat{A}_\mu$ and the free photon field $\hat{A}_\mu$ in the Coulomb (radiation) gauge can be written as

$$\hat{A}_\mu(x) = \int \frac{d^3\mathbf{k}}{(2\pi)^3 2k^0}[\hat{a}_r(k)\epsilon_{r\mu}(k)e^{-ik.x} + \hat{a}_r^\dagger(k)\epsilon_{r\mu}^*(k)e^{ik.x}], \tag{32}$$

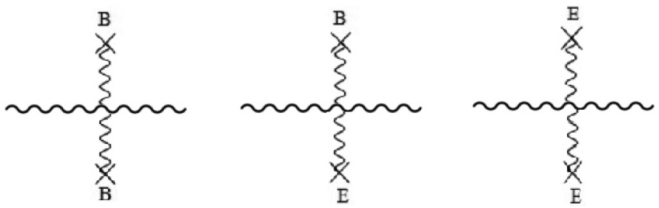


FIG. 1. Photon-photon interactions in the background of electromagnetic fields, where B represents the classical magnetic field and E represents the classical electric field.

where $\epsilon_{r\mu}(k) = (0,\vec{\epsilon}_r(k))$; $r = 1,2$ shows the photon polarization four-vectors for the two orthogonal transverse polarizations; and $k$ (with $k^0 = |\mathbf{k}|$) stands for the four-momentum. The creation and annihilation operators satisfy the canonical commutation relation as

$$[\hat{a}_i(k),\hat{a}_j^{\dagger}(k')] = (2\pi)^3 2k^0\delta_{ij}\delta^{(3)}(\mathbf{k}-\mathbf{k}'). \tag{33}$$

We compute the evolution of the density matrix and the Stokes parameters in the effective Euler-Heisenberg (31) framework and in the presence of background fields. We only consider the leading term (forward scattering) in the Boltzmann equation (30) as follows:

$$(2\pi)^3 2k^0\delta^{(3)}(0)\frac{d}{dt}\rho_{ij}(\mathbf{k}) = i\langle[\hat{\mathcal{H}}_{\rm int}(t),\hat{\mathcal{D}}_{ij}(\mathbf{k})]\rangle. \tag{34}$$

Regarding the canonical commutation relations of the creation and annihilation operators and their expectation values given in [24] it is easy to see that the nonvanishing contribution to the right-hand side of Eq. (34) comes from the photon interaction with two background field $F_{\mu\nu}$ as shown in Fig. 1. The interaction with three background fields has no contribution to the term $\langle[\hat{\mathcal{H}}_{\rm int}(t)\hat{\mathcal{D}}_{ij}(\mathbf{k})]\rangle$ of Eq. (34), because we have ignored correlations such as $\langle\hat{a}_i(k)\hat{a}_j(k')\rangle$ and $\langle\hat{a}_i^{\dagger}(k)\hat{a}_j^{\dagger}(k')\rangle$. In fact, we are assuming that the background field $F_{\mu\nu}$ varies slowly enough in time so that physical two-photon states are neither created nor destroyed by the interaction. In this case the nonlinear interacting part of the Lagrangian (31) can be found as follows:

$$\begin{aligned}\mathcal{L}_{\rm int} = \frac{\alpha^2}{90m_e^4}[&5f_{\mu\nu}f^{\mu\nu}F_{\lambda\rho}F^{\lambda\rho} + 10F_{\mu\nu}f^{\mu\nu}f_{\lambda\rho}F^{\lambda\rho}\\ &- 14f_{\mu\nu}F^{\nu\lambda}f_{\lambda\rho}F^{\rho\mu} - 28f_{\mu\nu}f^{\nu\lambda}F_{\lambda\rho}F^{\rho\mu}].\end{aligned} \tag{35}$$

By substituting Eq. (32) into Eq. (35) and using the coulomb gauge ($\hat{\epsilon}\cdot\hat{k} = 0$), one can calculate $\mathcal{H}_{\rm int} = -\int d^3x\mathcal{L}_{\rm int}$ as follows:

$$\begin{aligned}\mathcal{H}_{\rm int} = \frac{2\alpha^2}{90m_e^4}\Bigg[\int\frac{d^3k}{(2\pi)^3(2k^0)^2}\sum_{ss'}\hat{a}_s^{\dagger}(k)\hat{a}_{s'}(k)\\ \times\left(12k^{\mu}F_{\mu\nu}\epsilon_{s'}^{\nu}k^{\lambda}F_{\lambda\rho}\epsilon_s^{*\rho} + 28k^{\lambda}F_{\lambda\rho}F^{\rho\mu}k_{\mu}\right)\Bigg].\end{aligned} \tag{36}$$

According to this interaction, the background field $F_{\mu\nu}$ behaves as an effective coupling between photons. In other words the photons interact with each other via background fields. We now proceed to evaluate $\langle[\mathcal{H}_{\rm int}^{B,2}(t),\hat{\mathcal{D}}_{ij}(\mathbf{k})]\rangle$ by using the contraction relation:

$$\langle\hat{a}_{s'}^{\dagger}(k')\hat{a}_s(k)\rangle = 2k^0(2\pi)^3\delta^3(\mathbf{k}-\mathbf{k}')\rho_{s's}(\mathbf{k}). \tag{37}$$

There is no contribution from the second part of Eq. (36) which contains only the background fields. Consequently the time evolution for the density matrix Eq. (34) can be obtained as follows:

$$\begin{aligned}\frac{d\rho_{ij}}{dt} = \frac{2i\alpha^2}{15k^0m_e^4}\Bigg[&\sum_s\left(k^{\mu}F_{\mu\nu}\epsilon_s^{\nu}\,k^{\lambda}F_{\lambda\rho}\epsilon_i^{*\rho}\right)\rho_{sj}\\ &-\left(k^{\mu}F_{\mu\nu}\epsilon_j^{\nu}\,k^{\lambda}F_{\lambda\rho}\epsilon_s^{*\rho}\right)\rho_{is}\Bigg].\end{aligned} \tag{38}$$

In the following, we choose $\vec{k} = k_0\hat{k}$, where $\hat{k}$ indicates the direction of outgoing photons from the transverse probe laser. We use the transverse condition for real polarization vectors, $\vec{\epsilon}_1(k)$ and $\vec{\epsilon}_2(k)$ being orthogonal to the direction of $\vec{k}$. The background antisymmetric field tensor $F_{\mu\nu}$ is expressed in terms of electric- and magnetic-field components

$$F_{\mu\nu} = \begin{pmatrix} 0 & E_x & E_y & E_z\\ -E_x & 0 & B_z & -B_y\\ -E_y & -B_z & 0 & B_x\\ -E_z & B_y & -B_x & 0\end{pmatrix}. \tag{39}$$

The magnetic-field components can be represented as a vector field $\vec{B} = F_{23}\hat{x} + F_{31}\hat{y} + F_{12}\hat{z}$; then we can proceed to the calculation, for example, the term $k^iF_{ij}\epsilon_s^j$ in Eq. (38):

$$\begin{aligned}k^iF_{ij}\epsilon_s^j &= F_{12}\left(k^1\epsilon_s^2 - k^2\epsilon_s^1\right) + F_{23}\left(k^2\epsilon_s^3 - k^3\epsilon_s^2\right)\\ &\quad + F_{31}\left(k^3\epsilon_s^1 - k^1\epsilon_s^3\right)\\ &= \vec{B}\cdot(\vec{k}\times\hat{\epsilon}_s).\end{aligned} \tag{40}$$

Also the electric-field components can be represented as a vector field $\vec{E} = F_{01}\hat{x} + F_{02}\hat{y} + F_{03}\hat{z}$ and

$$k^0F_{0i}\epsilon_s^i = k^0\left(F_{01}\epsilon_s^1 + F_{02}\epsilon_s^2 + F_{03}\epsilon_s^3\right) = k^0\vec{E}\cdot\hat{\epsilon}_s. \tag{41}$$

As a result the time derivative components of the density matrix can be expressed as

$$\begin{aligned}\frac{d\rho_{ij}}{dt} = \frac{2i\alpha^2k^0}{15m_e^4}\Bigg[&\sum_s(\vec{B}\cdot(\hat{k}\times\hat{\epsilon}_s)\,\vec{B}\cdot(\hat{k}\times\hat{\epsilon}_i) + \vec{E}\cdot\hat{\epsilon}_s\vec{B}\cdot(\hat{k}\times\hat{\epsilon}_i) + \vec{E}\cdot\hat{\epsilon}_i\vec{B}\cdot(\hat{k}\times\hat{\epsilon}_s) + \vec{E}\cdot\hat{\epsilon}_i\vec{E}\cdot\hat{\epsilon}_s)\rho_{sj}\\ &-(\vec{B}\cdot(\hat{k}\times\hat{\epsilon}_j)\,\vec{B}\cdot(\hat{k}\times\hat{\epsilon}_s) + \vec{E}\cdot\hat{\epsilon}_j\vec{B}\cdot(\hat{k}\times\hat{\epsilon}_s) + \vec{E}\cdot\hat{\epsilon}_s\vec{B}\cdot(\hat{k}\times\hat{\epsilon}_j) + \vec{E}\cdot\hat{\epsilon}_j\vec{E}\cdot\hat{\epsilon}_s)\rho_{is}\Bigg]\end{aligned} \tag{42}$$

the components of which are

$$\dot{\rho}_{11} = \frac{2i\alpha^2 k^0}{15m_e^4}[(\vec{B}\cdot(\hat{k}\times\hat{\epsilon}_2)\,\vec{B}\cdot(\hat{k}\times\hat{\epsilon}_1) + \vec{E}\cdot\hat{\epsilon}_2\vec{B}\cdot(\hat{k}\times\hat{\epsilon}_1) + \vec{E}.\hat{\epsilon}_1\vec{B}\cdot(\hat{k}\times\hat{\epsilon}_2) + \vec{E}\cdot\hat{\epsilon}_1\vec{E}\cdot\hat{\epsilon}_2)(\rho_{21}-\rho_{12})], \quad (43)$$

$$\dot{\rho}_{22} = \frac{2i\alpha^2 k^0}{15m_e^4}[(\vec{B}\cdot(\hat{k}\times\hat{\epsilon}_2)\,\vec{B}\cdot(\hat{k}\times\hat{\epsilon}_1)+\vec{E}\cdot\hat{\epsilon}_2\vec{B}\cdot(\hat{k}\times\hat{\epsilon}_1) + \vec{E}\cdot\hat{\epsilon}_1\vec{B}\cdot(\hat{k}\times\hat{\epsilon}_2) + \vec{E}\cdot\hat{\epsilon}_1\vec{E}\cdot\hat{\epsilon}_2)(\rho_{12}-\rho_{21})], \quad (44)$$

$$\dot{\rho}_{12} = \frac{2i\alpha^2 k^0}{15m_e^4}[(\vec{B}\cdot(\hat{k}\times\hat{\epsilon}_2)\,\vec{B}\cdot(\hat{k}\times\hat{\epsilon}_1)+\vec{E}\cdot\hat{\epsilon}_2\vec{B}\cdot(\hat{k}\times\hat{\epsilon}_1) + \vec{E}\cdot\hat{\epsilon}_1\vec{B}\cdot(\hat{k}\times\hat{\epsilon}_2) + \vec{E}\cdot\hat{\epsilon}_1\vec{E}\cdot\hat{\epsilon}_2)(\rho_{22}-\rho_{11}) + ((\vec{B}\cdot\hat{k}\times\hat{\epsilon}_1+\vec{E}\cdot\hat{\epsilon}_1)^2-(\vec{B}\cdot\hat{k}\times\hat{\epsilon}_2+\vec{E}\cdot\hat{\epsilon}_2)^2)\rho_{12}], \quad (45)$$

$$\dot{\rho}_{21} = \frac{2i\alpha^2 k^0}{15m_e^4}[(\vec{B}\cdot(\hat{k}\times\hat{\epsilon}_2)\,\vec{B}\cdot(\hat{k}\times\hat{\epsilon}_1) + \vec{E}\cdot\hat{\epsilon}_2\vec{B}\cdot(\hat{k}\times\hat{\epsilon}_1) + \vec{E}\cdot\hat{\epsilon}_1\vec{B}\cdot(\hat{k}\times\hat{\epsilon}_2) + \vec{E}\cdot\hat{\epsilon}_1\vec{E}\cdot\hat{\epsilon}_2)(\rho_{11}-\rho_{22}) + ((\vec{B}\cdot\hat{k}\times\hat{\epsilon}_2+\vec{E}\cdot\hat{\epsilon}_2)^2-(\vec{B}\cdot\hat{k}\times\hat{\epsilon}_1+\vec{E}\cdot\hat{\epsilon}_1)^2)\rho_{21}]. \quad (46)$$

Hence the time evolution of the Stokes parameters is

$$\dot{I} = \dot{\rho}_{11} + \dot{\rho}_{22} = 0, \quad (47)$$

$$\dot{Q} = \dot{\rho}_{11} - \dot{\rho}_{22} = -\frac{4\alpha^2 k^0}{15m_e^4}[(\vec{B}\cdot(\hat{k}\times\hat{\epsilon}_2)\,\vec{B}\cdot(\hat{k}\times\hat{\epsilon}_1) + \vec{E}\cdot\hat{\epsilon}_2\vec{B}\cdot(\hat{k}\times\hat{\epsilon}_1) + \vec{E}\cdot\hat{\epsilon}_1\vec{B}\cdot(\hat{k}\times\hat{\epsilon}_2) + \vec{E}\cdot\hat{\epsilon}_1\vec{E}\cdot\hat{\epsilon}_2)]V, \quad (48)$$

$$\dot{U} = \dot{\rho}_{21} + \dot{\rho}_{12} = -\frac{2\alpha^2 k^0}{15m_e^4}[(\vec{B}\cdot\hat{k}\times\hat{\epsilon}_2+\vec{E}\cdot\hat{\epsilon}_2)^2 - (\vec{B}\cdot\hat{k}\times\hat{\epsilon}_1+\vec{E}\cdot\hat{\epsilon}_1)^2]V, \quad (49)$$

$$\dot{V} = i(\dot{\rho}_{12} - \dot{\rho}_{21}) = \frac{2\alpha^2 k^0}{15m_e^4}[2(\vec{B}\cdot(\hat{k}\times\hat{\epsilon}_2)\,\vec{B}.(\hat{k}\times\hat{\epsilon}_1) + \vec{E}\cdot\hat{\epsilon}_2\vec{B}\cdot(\hat{k}\times\hat{\epsilon}_1) + \vec{E}\cdot\hat{\epsilon}_1\vec{B}\cdot(\hat{k}\times\hat{\epsilon}_2) + \vec{E}\cdot\hat{\epsilon}_1\vec{E}\cdot\hat{\epsilon}_2)Q + ((\vec{B}\cdot\hat{k}\times\hat{\epsilon}_2+\vec{E}\cdot\hat{\epsilon}_2)^2-(\vec{B}\cdot\hat{k}\times\hat{\epsilon}_1+\vec{E}\cdot\hat{\epsilon}_1)^2)]U. \quad (50)$$

Equation (47) tells us that, in the photon ensemble, the total intensity of photons does not depend on the photon-photon forward-scattering term. According to Eqs. (48)–(50), the unpolarized photons (namely, $Q = U = V = 0$) cannot acquire any polarization during propagating through the background fields. In contrast, linear polarized photons (namely, $Q$ and/or $U \neq 0$) can acquire circular polarization $V \neq 0$ [see Eq. (50)]. We recall that the generation of circular polarizations from linearly polarized laser beam collisions due to the Euler-Heisenberg effective Lagrangian was discussed in [22].

## IV. ANALYTICAL AND NUMERICAL SOLUTIONS

In the last section we investigated the generation of circular polarization in the presence of strong background fields. Here we attempt to consider two cases. The strong background field is made by (i) an ultraintense laser pulse (time-dependent fields) and (ii) superconductor magnets (static fields). The time evolution of Stokes parameters (47)–(50) can be rewritten as below:

$$\dot{I} = 0, \quad \dot{Q} = -\Omega_{QV}V, \quad \dot{U} = -\Omega_{UV}V, \quad \dot{V} = \Omega_{QV}Q + \Omega_{UV}U, \quad (51)$$

$$\Omega_{QV} = \frac{4\alpha^2 k^0}{15m_e^4}[(\vec{B}\cdot(\hat{k}\times\hat{\epsilon}_2)\,\vec{B}\cdot(\hat{k}\times\hat{\epsilon}_1) + \vec{E}\cdot\hat{\epsilon}_2\vec{B}\cdot(\hat{k}\times\hat{\epsilon}_1) + \vec{E}\cdot\hat{\epsilon}_1\vec{B}\cdot(\hat{k}\times\hat{\epsilon}_2) + \vec{E}\cdot\hat{\epsilon}_1\vec{E}\cdot\hat{\epsilon}_2)], \quad (52)$$

$$\Omega_{UV} = \frac{2\alpha^2 k^0}{15m_e^4}[(\vec{B}.\hat{k}\times\hat{\epsilon}_2+\vec{E}.\hat{\epsilon}_2)^2 - (\vec{B}.\hat{k}\times\hat{\epsilon}_1+\vec{E}.\hat{\epsilon}_1)^2]. \quad (53)$$

From these equations we have

$$\ddot{V} = -\Omega^2 V + \dot{\Omega}_{QV}Q + \dot{\Omega}_{UV}U, \quad (54)$$

$$\Omega^2 = \Omega_{QV}^2 + \Omega_{UV}^2. \quad (55)$$

From Eq. (51) it is easy to show $Q\dot{Q} + U\dot{U} + V\dot{V} = 0$, and the relation between Stokes parameters ($I^2 = Q^2 + U^2 + V^2$) is automatically satisfied.

### A. Analytical solution in the presence of a time-independent background field

In the case of time-independent background fields, the $\Omega_{QV}$ and $\Omega_{UV}$ are constant in time, and Eq. (54) becomes a simple harmonic equation $\ddot{V} + \Omega^2 V = 0$ which has a general solution

$$V(t) = \mathcal{A}\sin(\Omega t) + \mathcal{B}\cos(\Omega t). \quad (56)$$

The coefficients $\mathcal{A}$ and $\mathcal{B}$ are determined by initial conditions at $t = 0$:

$$V(0) = \mathcal{B}, \quad \dot{V}(0) = \mathcal{A}\Omega = \Omega_{QV}Q(0) + \Omega_{UV}U(0). \quad (57)$$

It is clear from Eq. (57) that $\dot{V}(0)$ is determined by linear polarization parameters $Q(0)$ and $U(0)$. $Q(t)$ and $U(t)$ can be found by adopting Eqs. (51) and (56) as follows:

$$\dot{Q} = -\Omega_{QV}V \Longrightarrow Q(t) = \frac{\Omega_{QV}}{\Omega}[\mathcal{A}\cos(\Omega t) - \mathcal{B}\sin(\Omega t)], \quad (58)$$

$$\dot{U} = -\Omega_{UV}V \Longrightarrow U(t) = \frac{\Omega_{UV}}{\Omega}[\mathcal{A}\cos(\Omega t) - \mathcal{B}\sin(\Omega t)]. \quad (59)$$

We supposed a totally linear polarized incoming radiation with $P_0 = 1$ ($Q_0 = U_0 = 1/\sqrt{2}$) without any initial circular

polarization ($V_0 = 0$); then the time evolution of Stokes parameters is given by

$$V(t) = \sin(\Omega t), \quad U(t) = Q(t) = \frac{1}{\sqrt{2}}\cos(\Omega t). \tag{60}$$

The final results in the time-independent background field show that the Stokes parameters are harmonically oscillating in time. This means that we should not expect any circular component after a long time with respect to the period $\Omega^{-1}$. However, one could measure the time average of squared total linear polarization $\langle P^2\rangle = \langle Q^2\rangle + \langle U^2\rangle = 1$ after several periods. The frequency $\Omega$ of these oscillations can be estimated in a real experimental setup like PVLAS (polarizzazione del vuoto con laser) experiments [7–9], where a linear polarized laser beam with a wavelength of 1064 nm propagates through a static magnetic field of about 2.5 T, the direction of which is orthogonal to the laser beam direction. With the help of Eqs. (52), (53), and (55) we have

$$\Omega = \frac{2\alpha^2 k^0 B_0^2}{15 m_e^4} = \frac{\alpha}{15\lambda_0}\left(\frac{eB_0}{m_e^2}\right)^2 = 4.43\times 10^{-8}\ \mathrm{s}^{-1}. \tag{61}$$

Then the period $T = 1.12\times 10^8$ s for one period or corresponding to the length $L = 3.36\times 10^{16}$ m. However, the magnets of the PVLAS experiment have a total magnetic field length $L = 1.6$ m, where $L$ is the optical path length within the birefringent region. This means that the oscillating effect [Eq. (60)] does not appear in the PVLAS like experiments. Let us determine the ellipticity signal by using Eqs. (20) and (60):

$$\begin{aligned}\epsilon_{\mathrm{QED}} &= \frac{1}{2}\tan^{-1}\left(\frac{\sin(\Omega t)}{\cos(\Omega t)}\right)\\ &= \frac{\Omega t}{2} = \frac{\alpha}{30}\left(\frac{eB}{m_e^2}\right)^2\frac{L}{\lambda_0} = 1.18\times 10^{-16}.\end{aligned} \tag{62}$$

This value of the ellipticity is very far from our current detector's precision. We note that the optical path length can be increased by using a Fabry-Perot cavity of finesse $\mathcal{F}$ as discussed in [9], where one can define the effective path length $\mathrm{L_{eff}} = \frac{2\mathcal{F}L}{\pi}$. With finesses $\mathcal{F} > 400\,000$ the value of the ellipticity signal can be increased up to $10^{-11}$. We use Eqs. (19) and (60) to obtain the rotation of the polarization plane:

$$\psi_{\mathrm{QED}} = \frac{1}{2}\tan^{-1}\left(\frac{U}{Q}\right) = \frac{1}{2}\tan^{-1}(1) \implies \dot{\psi}_{\mathrm{QED}} = 0. \tag{63}$$

These results confirm previous studies [10,20,31,32], which are mainly based on the semiclassical approach (viewing fields as classical fields) and evaluation of one loop polarization tensor. Our approach is based on using the quantum Boltzmann equation to determine all the Stokes parameters regarding the quantum structure of a probe beam. In contrast to previous consideration where the assumption of the constant background field has been used to extract the photon polarization tensor from the Euler-Heisenberg Lagrangian, our method can be easily extended to time-dependent background fields (see Sec. IV B).

It is clear from Eq. (63) that the nonlinear QED interactions through the Euler-Heisenberg Lagrangian cannot rotate the linear polarization plane for a laser beam traversing a static magnetic field. Regarding Eq. (13) the rotation angle $\psi$ of an initially linear polarized photon is due to the imaginary part of the refractive index ($\tilde{n} = n + i\kappa$). The effects which modify the light amplitudes in the different directions will induce a rotation angle. Those effects cannot be explained in QED below the threshold ($\omega < 2m_e$) where the electron-positron pair production rate is exponentially suppressed and further possibilities such as photon splitting [31] or neutrino-pair production [33] are unmeasurably small. In other words QED does not predict dichroism. Therefore, a non-negligible signal for vacuum rotation angle $\psi$ may imply evidence for new physics beyond the standard model of particle physics. This could be interpreted as a neutral scalar or pseudoscalar particle weakly coupling to two photons called axionlike particles (ALPs) [34,35] or other candidates such as millicharged particles (MCPs) [36,37]. It is worth mentioning that an observation of the rotation of the polarization plane by the vacuum in a static magnetic field was reported by the PVLAS group in 2006 [38]; they announced the existence of a very light, neutral, spin-zero particle coupled to two photons, while this observation was excluded by data taken with an upgraded setup in 2008 [7].

### B. Numerical solution in the case of two laser beam collisions

In this section, we want to consider collision of two laser beams. Assuming that the linearly polarized probe beam passes through another laser beam with lower frequency, the latter is considered as a background field. Consider the collision of two linearly polarized laser pulses, a low-intensity x-ray probe pulse $(\hat{k},\hat{\epsilon}_1(k),\hat{\epsilon}_2(k))$ crossing the high-intensity optical pulse $(\hat{p},\hat{E}(p),\hat{B}(p))$ as a target beam. Due to the separation in energy scales the probe beam essentially scatters forward. Here in contrast to the previous section the background fields vary with time. The electric and magnetic fields are oscillating, their amplitudes are related to each other by $|E| = |B|$, and directions are orthogonal to the beam direction:

$$\hat{k} = \begin{pmatrix}0\\0\\1\end{pmatrix}, \quad \hat{\epsilon}_1(k) = \begin{pmatrix}1\\0\\0\end{pmatrix}, \quad \hat{\epsilon}_2(k) = \begin{pmatrix}0\\1\\0\end{pmatrix}, \tag{64}$$

and

$$\begin{aligned}\hat{p} &= \begin{pmatrix}\sin\theta\cos\phi\\ \sin\theta\sin\phi\\ \cos\theta\end{pmatrix}, \quad \hat{E}(p) = \sin\omega t\begin{pmatrix}\cos\theta\cos\phi\\ \cos\theta\sin\phi\\ -\sin\theta\end{pmatrix},\\ \hat{B}(p) &= \cos\omega t\begin{pmatrix}-\sin\phi\\ \cos\phi\\ 0\end{pmatrix},\end{aligned} \tag{65}$$

where $\hat{k}$, $\hat{\epsilon}_1$, and $\hat{\epsilon}_2$ are momentum and polarization unit vectors of the incident (probe) beam; $\hat{p}$, $\hat{E}$, and $\hat{B}$ are momentum, electric-field, and magnetic-field unit vectors of the target laser beam ($\vec{E} = E_0\hat{E}, \vec{B} = B_0\hat{B}$). Regarding Eqs. (64) and (65) for

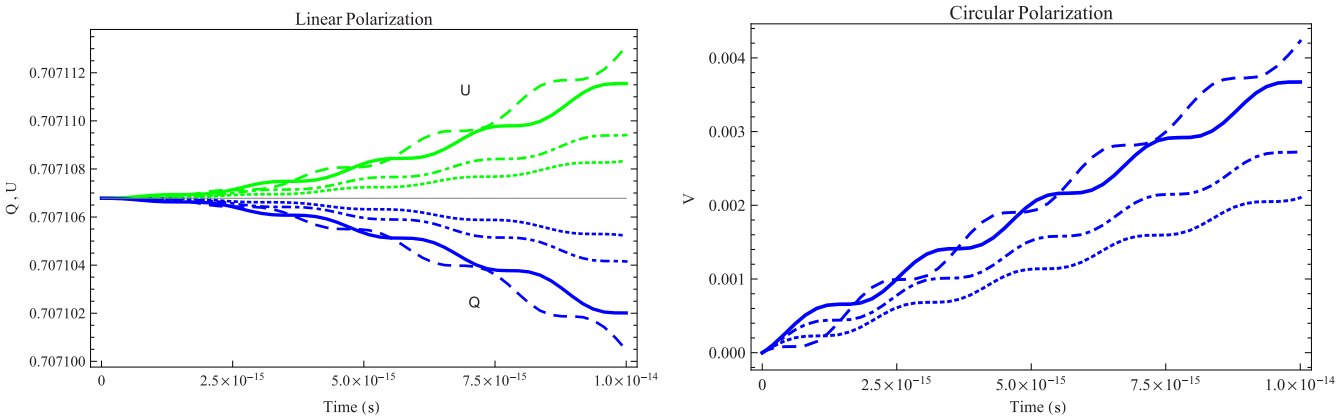


FIG. 2. In the left panel, the time evolution of dimensionless Stokes parameters $U$ [upper half plane (green)] and $Q$ [lower half plane (blue)]. In the right panel, the time evolution of dimensionless Stokes parameter $V$. They are plotted for a 10-keV linearly polarized probe laser beam interacting with a target laser beam in optical frequency $\omega = 1$ eV and peak intensity $I = 3 \times 10^{22}$ W/cm$^2$. These figures show the impact of collision geometry for two laser beams on the evolution of Stokes parameters, for different polar angles $\theta = \pi$ (dashed lines), $\pi/2$ (dotted lines), $\pi/3$ (dot-dashed lines), and $\pi/5$ (solid lines) at a fixed azimuthal angle $\phi = \pi/8$.

$\Omega_{QV}$ and $\Omega_{UV}$ we obtain

$$\Omega_{QV} = G \sin 2\phi[\cos^2 \omega t + \sin 2\omega t \cos\theta + \sin^2 \omega t \cos^2\theta], \tag{66}$$

$$\Omega_{UV} = -G \cos 2\phi[\cos^2 \omega t + \sin 2\omega t \cos\theta + \sin^2 \omega t \cos^2\theta], \tag{67}$$

where

$$G = \left[\frac{2\alpha^2 k^0 B_0^2}{15 m_e^4}\right] = \frac{2.99\alpha}{15}\left[\frac{\mathrm{I}}{\mathrm{I}_c}\right]\left[\frac{1\ \mathrm{nm}}{\lambda_0}\right] \times 10^{20}\ \mathrm{s}^{-1}$$
$$= 1.45\left[\frac{\mathrm{I}}{\frac{\mathrm{W}}{\mathrm{cm}^2}}\right]\left[\frac{1\ \mathrm{nm}}{\lambda_0}\right] \times 10^{-12}\ \mathrm{s}^{-1}. \tag{68}$$

We assume that the background field is an intense and focused laser beam in optical frequency $\omega = 1$ eV, and this optical petawatt laser has the peak intensity $I = P/\pi d^2 \simeq 3 \times 10^{22}$ W/cm$^2$ (power $P = 1$ PW and pulse length $d = 1\ \mu$m). It should be noted that $(eB)^2 = (\mathrm{I}/\mathrm{I}_c)(eB)_c^2$ where $I_c = 10^{29}$ W/cm$^2$ and $(eB)_c = m_e^2 = 1.282 \times 10^{13}$ G. Let us assume the probe beam is an XFEL, with $\lambda$=0.1-nm wavelength, hence $k^0 = h\nu^0 = 10$ keV, like the DESY project [5]. At x-ray photon energies of the order of 10 keV, the highest polarization purities can be achieved by reflection at perfect crystals at a Bragg angle of $\pi/4$ [39]. This x-ray probe beam can also be achieved experimentally from a laser-based Thomson back-scattering source [20]. It has been supposed that the initial value of the circular polarization $V_0 = 0$ and the linear polarization $P_0 = \sqrt{Q_0^2 + U_0^2} = 1$ ($Q_0 = U_0 = 1/\sqrt{2}$), which are all dimensionless quantities. The Stokes parameters are normalized by the intensity $I$, giving the dimensionless quantities. Using this set of parameters we solved Eqs. (51) and determined the time evolution of the Stokes parameters followed by ellipticity and polarization rotation angles. The results for various polar angles ($\theta$) of two beams' direction in a fixed azimuthal angle $\phi = \pi/8$ are displayed in Figs. 2 and 3. These figures show the polarization evolution of an x-ray probe beam as a result of interacting with the optical laser field in the crossing region of two laser beams. The interaction time is limited by the pulse length $d = 1\ \mu$m. As one can find from Fig. 2 (right panel), the circular polarization $V$ gets its maximum value for the head-on collision of the two laser beams ($\theta = \pi$), and its minimum value for the transverse collision angle ($\theta = \pi/2$). From Fig. 2 (left panel), it is obvious that $U$ increases with time although $Q$ decreases with time;

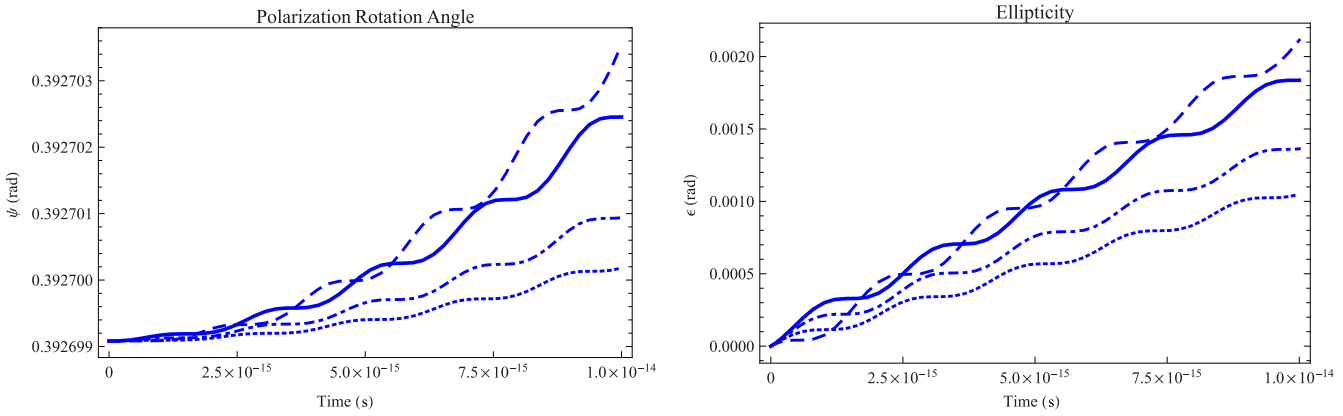


FIG. 3. The polarization rotation angle $\Psi$ (left) and the ellipticity parameter $\epsilon$ as a function of time (right) for the cases depicted in Fig. 2.

according to Eqs. (51), the change of $Q$ and $U$ with time acts as a source term for circular polarization parameter $V$.

In the presence of time-dependent background field, the governing equation of Stokes parameter $V$ is not a simple harmonic equation [see Eq. (54)], since $\Omega_{QV}$ and $\Omega_{UV}$ of Eqs. (66) and (67) are time-dependent quantities in this case. In the laser-laser collision $U/Q$ is a function of time as a result of time-dependent configuration in the interaction region which leads to a time-evolving rotation angle $\psi_{\rm QED}(t)$:

$$\frac{\dot{U}}{\dot{Q}} = \frac{\Omega_{UV}(t)}{\Omega_{QV}(t)} \implies \dot{\psi}_{\rm QED} = \frac{d}{dt}\left[\frac{1}{2}\tan^{-1}\left(\frac{U}{Q}\right)\right] \neq 0. \tag{69}$$

This result is different from what we obtained in the propagation of a laser beam in the static magnetic field of PVLAS-like experiments [see Eq. (63)]. The rotation angle of the polarization plane acquired by a probe beam via a crossing region of size 1 $\mu$m is $\Delta\psi \sim 4.5 \times 10^{-6}$ rad in the head-on collision ($\theta = \pi$), as shown in Fig. 3 (left panel). This result is considered here in QED below the threshold energy of pair production. Our approach provides an explanation for vacuum rotation within the framework of QED in the presence of a time-dependent background field. Therefore, it shows us that any sizable signal of the vacuum rotation angle $\psi$ in the strong-field regime is not essentially a signature of new physics (ALPs and MCPs). Besides, Fig. 3 (right panel) shows that the maximum value of the ellipticity $\epsilon$ acquired by probe photons in the above-mentioned interaction length is $2 \times 10^{-3}$ rad, which is three orders of magnitude larger than the rotation angle. Moreover the light diffraction by a strong standing electromagnetic wave also leads to vacuum rotation but for pure kinematical reasons, depending on the details of the optical setup [13,21]. This is different from the laser-laser collisions which we are considering here. The rotation angle found in [21] is the same order of magnitude as the induced ellipticity. Thanks to recent technological advances in x-ray polarimetry [39], the x-ray polarimeters allow detection of rotation of the polarization plane down to 1 arc sec ($4.8 \times 10^{-6}$ rad) and ellipticities of about $1.51 \times 10^{-5}$ rad. Recently, authors in [40] presented a comprehensive study of the feasibility of measuring vacuum birefringence by probing the focus of a high intensity optical laser with an x-ray free-electron laser.

In this paper our computations are based on perfect vacuum assumption; actually the presence of charged particles in the interaction region may obscure the measurement of real photon-photon scattering [41]. Since in the presence of an electromagnetic wave a gas becomes a birefringent medium due to the Cotton-Mouton and Kerr effects [7,42], it is compulsory to clean the interaction region by removing all residual gas particles to avoid an additional background signal. Fortunately, because of the small interaction region in the laser-laser collision, the absence of residual particles is only required for a short time period [40].

## V. POLARIZATION OF A PROBE LASER BEAM IN TIME-DEPENDENT AND STATIC BACKGROUND FIELDS

In this section, we attempt to clarify the differences between using a static magnetic field and time-dependent fields that induce polarization characteristics of a given probe laser beam. We assume a 10-keV probe laser beam with initial Stokes parameters $Q_0 = U_0 = 1/\sqrt{2}$ and $V_0 = 0$, and an optical target laser beam with intensity $I = 3 \times 10^{22}$ W/cm$^2$ and frequency $\omega = 1$ eV. For the time-dependent fields which are realized in the cross section of laser beams, we used Eqs. (51) and (64)–(67) with $\theta = \pi$ (head-on collision) and $\phi = \frac{\pi}{8}$, in which both electric and magnetic fields are perpendicular to the beam direction $\hat{k}$ ($\hat{E}, \hat{B} \perp \hat{k}$). For the static magnetic field $B = 7.02 \times 10^9$ G corresponding to the peak intensity of background optical laser $I = 3 \times 10^{22}$ W/cm$^2$, we used Eq. (60). In Fig. 4 we compare the evolution of Stokes parameters of the probe laser beam in these two cases (time-dependent and static background fields). Here, we plotted analytic solutions and numerical solutions of the Boltzmann equation for the same field intensity. Since interaction time is too short ($10^{-14}$ s), we can approximate Eqs. (60) up to first

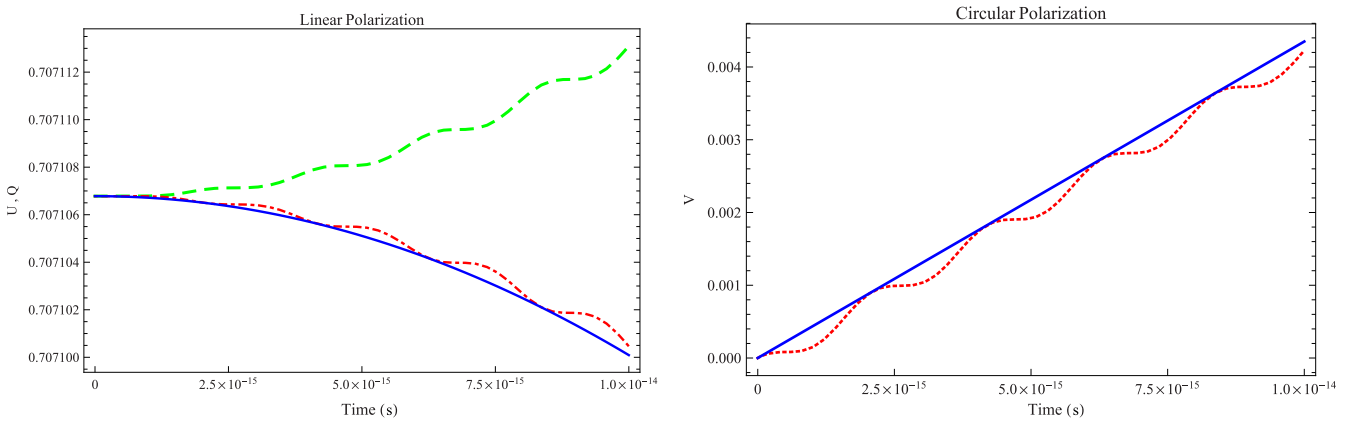


FIG. 4. Comparison between dimensionless Stokes parameters $U$, $Q$, and $V$ in both time-dependent and static background fields. In the time-dependent case we used the numerical solution of Sec. IV B to plot $U$ [dashed (green) line] and $Q$ [dot-dashed (red) line] in the left panel and for $V$ [dotted (red) line] in the right panel. In the static magnetic field we have used the analytic solution of Sec. IV A to plot $Q$ and $U$ [solid (blue) line] in the left panel and $V$ [solid (blue) line] in the right panel. These figures are plotted for a 10-keV linearly polarized probe laser beam interacting with a target laser beam in optical frequency $\omega = 1$ eV and peak intensity $I = 3 \times 10^{22}$ W/cm$^2$.

order in time as

$$V(t) = \sin(\Omega t) \approx \Omega t, \quad U(t) = Q(t) = \frac{1}{\sqrt{2}}\cos(\Omega t) \approx \frac{1}{\sqrt{2}}. \tag{70}$$

This approximation shows us that $V$ varies faster than $Q$ and/or $U$ in a very short period of time. It helps us to explain three order-of-magnitude differences between ellipticity $\epsilon$ and polarization angle $\psi$ in the numerical solutions of laser-laser collision (Sec. IV B). As shown in Fig. 4 (left panel), in the static field there is not any conversion between $U$ and $Q$, and then polarization angle will not change during propagation in such a static field, and the value of the $V$ parameter (right panel) in the presence of a time-dependent background field oscillates around the value in the static case.

## VI. CONCLUSIONS AND REMARKS

Due to the extremely large value of the critical field it remains very challenging to experimentally verify QED nonlinearities, by exploring polarization characteristics of the laser photon propagation in the static and uniform magnetic field. As mentioned in this paper, much stronger electromagnetic fields can be produced by means of focused high-power lasers. We have discussed the polarization properties induced in a probe laser beam during its propagation through a constant magnetic field or in collision with another laser beam. We solved the quantum Boltzmann equation within the framework of the Euler-Heisenberg Lagrangian for both time-dependent and static background fields to explore the time evolution of Stokes parameters $Q$, $U$, and $V$ [see Eqs. (51)]. It is shown that the oscillating solution for the Stokes parameters in the static magnetic field has an oscillating period proportional to $k_0^{-1}B_0^{-2}$. The ellipticity signal can be increased up to $10^{-11}$ rad by using the cavity in the PVLAS experiment. Since it seems cavity techniques are inefficient for short pulsed high-intensity fields to produce a standing wave like what is proposed in [20,21], it is necessary to consider time-dependent background fields. For the time-dependent background field we considered laser-laser collisions. We have generalized the conditions of previous work [22] to the more realistic case of a temporal laser background probed by x-ray photon pulses. We obtained maximum ellipticity $\epsilon \sim 2 \times 10^{-3}$ rad and rotation of the polarization plane $\Delta\psi \sim 4.5 \times 10^{-6}$ rad, in the case of high-intensity background field $I = 3 \times 10^{22}$ W/cm$^2$ probed by 10-keV photon pulses. These values are at the limit of the accuracy that can now be obtained with high-contrast x-ray polarimeters using multiple Bragg reflections from channel-cut perfect crystals [39,40,43]. High-precision experiments using ultraintense lasers would be testing the most successful theory QED in the strong-field regime, which has been little explored so far. Beyond this, these experiments can shed light on the hidden sector of the standard model, and such a test will be sensitive to physics beyond the standard model [36,44,45].

## ACKNOWLEDGMENTS

S.S. is grateful to Prof. R. Ruffini for supporting his visit at ICRANet Pescara, where the last part of this work was done. He would like to thank R. Mohammadi, M. Haghighat, and C. Stahl for useful comments and discussions.

[1] H. Euler and B. Kockel, Die Naturwissenschaften **23**, 246 (1935).
[2] W. Heisenberg and H. Euler, Zeitschrift für Physik **98**, 714 (1936).
[3] V. Dinu, T. Heinzl, A. Ilderton, M. Marklund, and G. Torgrimsson, Phys. Rev. D **90**, 045025 (2014).
[4] F. Sauter, Zeitschrift für Physik **69**, 742 (1931).
[5] HIBEF website, http://www.hzdr.de/hibef.
[6] ELI, http://www.hzdr.de/hibef, "HiPER", http://www.hiperlaser.org, "XCELS", http://www.xcels.iapras.ru/img/XCELS-Project-english-version.pdf.
[7] E. Zavattini, G. Zavattini, G. Ruoso, G. Raiteri, E. Polacco, E. Milotti, V. Lozza, M. Karuza, U. Gastaldi, G. Di Domenico, F. Della Valle, R. Cimino, S. Carusotto, G. Cantatore, and M. Bregant (PVLAS Collaboration), Phys. Rev. D **77**, 032006 (2008).
[8] F. Della Valle, A. Ejlli, U. Gastaldi, G. Messineo, E. Milotti, R. Pengo, G. Ruoso, and G. Zavattini, Eur. Phys. J. C **76**, 24 (2016).
[9] F. Della Valle, U. Gastaldi, G. Messineo, E. Milotti, R. Pengo, L. Piemontese, G. Ruoso, and G. Zavattini, New J. Phys. **15**, 053026 (2013).
[10] W. Dittrich and H. Gies, in *Frontier Tests of QED and Physics of the Vacuum*, edited by E. Zavattini, D. Bakalov, and C. Rizzo (Heron Press, Sofia, Hungary, 1998), p. 29.
[11] A. di Piazza, C. Müller, K. Z. Hatsagortsyan, and C. H. Keitel, Rev. Mod. Phys. **84**, 1177 (2012).
[12] G. Torgrimsson, Few-Body Syst. **56**, 615 (2015).
[13] H. Gies, Eur. Phys. J. D **55**, 311 (2009).
[14] T. Heinzl and A. Ilderton, arXiv:0809.3348.
[15] T. Heinzl and A. Ilderton, Eur. Phys. J. D **55**, 359 (2009).
[16] V. Yanovsky, V. Chvykov, G. Kalinchenko, P. Rousseau, T. Planchon, T. Matsuoka, A. Maksimchuk, J. Nees, G. Cheriaux, G. Mourou, and K. Krushelnick, Opt. Express **16**, 2109 (2008).
[17] T. Heinzl and A. Ilderton, Opt. Commun. **282**, 1879 (2009).
[18] J. Schwinger, Phys. Rev. **82**, 664 (1951).
[19] R. Ruffini, G. Vereshchagin, and S.-S. Xue, Phys. Rep. **487**, 1 (2010).
[20] T. Heinzl, B. Liesfeld, K.-U. Amthor, H. Schwoerer, R. Sauerbrey, and A. Wipf, Opt. Commun. **267**, 318 (2006).
[21] A. Di Piazza, K. Z. Hatsagortsyan, and C. H. Keitel, Phys. Rev. Lett. **97**, 083603 (2006).
[22] R. Mohammadi, I. Motie, and S.-S. Xue, Phys. Rev. A **89**, 062111 (2014).
[23] S. Alexander, J. Ochoa, and A. Kosowsky, Phys. Rev. D **79**, 063524 (2009).
[24] A. Kosowsky, Ann. Phys. (NY) **246**, 49 (1996).
[25] W. D. Jackson, *Classical Electrodynamics* (Wiley, New York, 1975).
[26] A. Cooray, A. Melchiorri, and J. Silk, Phys. Lett. B **554**, 1 (2003).

[27] E. Collett, *Field Guide to Polarization* (SPIE, Bellingham, 2005).
[28] H. Euler, Ann. Phys. **418**, 398 (1936).
[29] D. A. Dicus, C. Kao, and W. W. Repko, Phys. Rev. D **57**, 2443 (1998).
[30] G. V. Dunne, Int. J. Mod. Phys. A **27**, 1260004 (2012).
[31] S. L. Adler, Ann. Phys. (NY) **67**, 599 (1971).
[32] J. S. Heyl and L. Hernquist, J. Phys. A **30**, 6485 (1997).
[33] H. Gies and R. Shaisultanov, Phys. Lett. B **480**, 129 (2000).
[34] L. Maiani, R. Petronzio, and E. Zavattini, Phys. Lett. B **175**, 359 (1986).
[35] M. Gasperini, Phys. Rev. Lett. **59**, 396 (1987).
[36] H. Gies, J. Jaeckel, and A. Ringwald, Phys. Rev. Lett. **97**, 140402 (2006).
[37] M. Ahlers, H. Gies, J. Jaeckel, and A. Ringwald, Phys. Rev. D **75**, 035011 (2007).
[38] E. Zavattini, G. Zavattini, G. Ruoso, E. Polacco, E. Milotti, M. Karuza, U. Gastaldi, G. Di Domenico, F. Della Valle, R. Cimino, S. Carusotto, G. Cantatore, and M. Bregant, Phys. Rev. Lett. **96**, 110406 (2006).
[39] B. Marx, K. S. Schulze, I. Uschmann, T. Kämpfer, R. Lötzsch, O. Wehrhan, W. Wagner, C. Detlefs, T. Roth, J. Härtwig, E. Förster, T. Stöhlker, and G. G. Paulus, Phys. Rev. Lett. **110**, 254801 (2013).
[40] H.-P. Schlenvoigt, T. Heinzl, U. Schramm, T. E. Cowan, and R. Sauerbrey, Phys. Scr. **91**, 023010 (2016).
[41] B. King and T. Heinzl, High Power Laser Science and Engineering **4**, e5 (2016).
[42] C. Rizzo, A. Rizzo, and D. M. Bishop, Int. Rev. Phys. Chem. **16**, 81 (2010).
[43] E. E. Alp, W. Sturhahn, and T. S. Toellner, Hyperfine Interact. **125**, 45 (2000).
[44] H. Gies, J. Phys. A **41**, 164039 (2008).
[45] R. Cameron, G. Cantatore, A. C. Melissinos, G. Ruoso, Y. Semertzidis, H. J. Halama, D. M. Lazarus, A. G. Prodell, F. Nezrick, C. Rizzo, and E. Zavattini, Phys. Rev. D **47**, 3707 (1993).